

---

# Training Data Protection with Compositional Diffusion Models

---

Aditya Golatkar   Alessandro Achille   Ashwin Swaminathan   Stefano Soatto  
AWS AI Labs  
{agolatka,aachille,swashwin,soattos}@amazon.com

## Abstract

We introduce Compartmentalized Diffusion Models (CDM), a method to train different diffusion models (or prompts) on distinct data sources and arbitrarily compose them at inference time. The individual models can be trained in isolation, at different times, and on different distributions and domains and can be later composed to achieve performance comparable to a paragon model trained on all data simultaneously. Furthermore, each model only contains information about the subset of the data it was exposed to during training, enabling several forms of training data protection. In particular, CDMs are the first method to enable both selective forgetting and continual learning for large-scale diffusion models, as well as allowing serving customized models based on the user’s access rights. CDMs also allow determining the importance of a subset of the data in generating particular samples.

## 1 Introduction

Diffusion models have captured the popular imagination by enabling users to generate compelling images using simple text prompts or sketches. They have also, in some cases, captured the personal workmanship of artists, since the sheer volume of training data makes it challenging to verify each sample’s attribution [57]. It is also challenging to quantify the data contribution in shaping the model’s generated output, which calls for the development

of new forms of protection for large-scale training data, ranging from methods that limit the influence of training samples *a-priori* (e.g., *differential privacy*), remove the influence of training examples that were wrongly included in the training *a-posteriori* (*selective forgetting*, *model disgorgement*), and limit the influence of samples on the training output (*copyright protection*), or at least identify which samples had the most influence (*attribution*), thus preventing memorization and/or generation of samples that are substantially similar to training data. While research in these fields is thriving, thus far the methods developed have not been shown to transfer to Diffusion Models, particularly in large-scale settings. Extending known techniques seems daunting since information from different samples is mixed irreversibly the weights of the model, making unlearning or evaluating the influence of specific data challenging.

We introduce Compartmentalized Diffusion Models (CDMs). In a CDM, separate parameters or prompts are trained independently on different data sources, ensuring perfect (deterministic) isolation of their respective information. All parameters are then merged at inference time and used jointly to generate samples. This technique is simple to implement with any existing DM architecture; CDMs are the first means to perform both selective forgetting and continual learning on large-scale diffusion models.

In addition to enabling the removal of information in the trained model from particular data, the method also allows attribution, which may inform the process of assessing the value of different

cohorts of training data, as well as ensure that there is no memorization so the generated images are not substantially similar to those used for training.

The key enabler of CDMs is a closed-form expression for the reverse diffusion flow of a mixture distribution in terms of the flows of its components. This expression is simple to derive and to implement with minimal changes to existing models, but it can suffer from two key problems. Implementation-wise, training and running separate models or adapters on different subsets of the data can quickly balloon the storage and inference costs of the model. Moreover, ensembling independent adapters trained on different subsets of the data can, in principle, significantly underperform a single model trained on all the data together, due to loss of synergistic information between samples [14].

To address the first problem, we propose an efficient method using prompt tuning, which can be easily implemented with Transformer-based diffusion models. The method is based on a single shared model and small prompts trained on each disjoint shard of the data. The prompts can be forwarded in parallel, taking advantage of efficient batch-parallelization for quick inference. Prompts can be trained remotely and shared with a central server without the need to share the raw data.

In regard to the latter problem, we empirically show that, in a variety of settings, a compartmentalized model can match the generative performance of a paragon model trained on all the data jointly, while allowing for all the above mentioned data security improvements. This is both due to the particular objective of diffusion models, which in theory allows separate model training without any loss in performance (even if this need not be the case for real models), and to our use of a *safe training set*, which allows the compartmentalized model components to still capture a significant amount of synergistic information [14].

## 2 Related Work

**Forgetting:** Forgetting or machine unlearning [18] studies the problem of removing information pertaining to training data from the weights of a trained machine learning model. There are two major directions of works in forgetting, the first direction [5, 58, 31, 34, 59] involves splitting the training dataset into multiple shards and training separate models on each shard. This ensures that the information contained in a particular training sample is restricted only to a specific subsets of parameters. When asked to remove a particular training sample, the unlearning procedure simply drops the corresponding shard and re-trains it without that sample. [58, 59, 31] proposed forgetting procedures which involves training adapters or single class classifiers using features from pre-trained models for different shards. This enables quicker training and removal of shards, compared to training the entire model. However, such shard based methods loose the synergistic information contained between different disjoint shards. To conquer this [14] proposed a method which first, partitions the dataset into a shard graph (graph with shards as nodes), and then trains adapters on different nodes of this shard graph. This enables the model to exploit the synergistic information while providing instant forgetting without compromising the model accuracy.

The second direction involves training a single machine learning model for the entire dataset, and providing approximate unlearning guarantees [21, 20, 19]. Such methods rely on the linearization [2] of the network with respect to a pre-trained initialization and then perform an approximate Newton step for forgetting [22, 24]. [41, 25, 55, 8, 48] provide stochastic algorithms for forgetting with theoretical guarantees similar to differential privacy [15].

**Diffusion Models:** Diffusion models are state-of-the-art generative models useful for high quality image generation [27, 50, 46, 11] which have completely outperformed generative adversarial networks [23], variational autoencoders [30] and its variants for image generation. They find varied application ranging from text-to-image generation [46, 45] to video generation [26, 40]. Diffusion models gradually add Gaussian noise to an image following a Markov process in the forward step, and perform denoising in the reverse step to generate data. [54] showed that the forward process in diffusion models can be modelled as a stochastic differential equation, whose reverse process is another stochastic differential equation. The reverse stochastic differential equation [42, 3] depends on the score [51, 53, 52] of the distribution which is learnt by the denoising diffusion models. This enables the use of stochastic differential solvers and probability flow equations for reverse diffusion. Improved diffusion solvers [38, 39, 29, 50] modify the stochastic differential equations corresponding to the reverse diffusion process to obtain not only improve sample quality, but also faster image generation. On another line, [37] recently proposed a conditional flow matching framework which

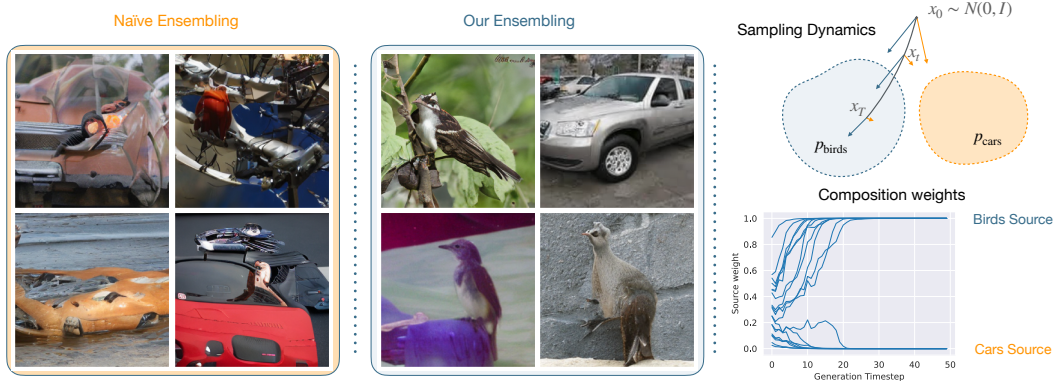


Figure 1: **Compositional diffusion models.** We train two diffusion models on two disjoint data distributions: Birds (CUB-200 [9]) and Stanford Cars [32]. (Left) Image generated by naively composing the models by averaging their output. The sample images are distorted and contain elements of both distributions within the same image. (Center) Sample images generated by our method using the same models. The quality is substantially higher and the samples do not conflate the two distributions. (Right) The key idea is illustrated graphically at each step of the reverse diffusion process, where we show the estimated optimal weights  $w_i$  to assign to each component. At the beginning, the two components are weighted equally, also shown in the plot below, but as the model approaches convergence, the weights increasingly favor only one of the two models, based on the likelihood that it was trained on a data distribution closest to the current sample.

subsumes diffusion models as a special case. Such models employ convolutional image-to-image transformation architectures [47] for denoising during reverse diffusion. [4] proposed a transformer based score model using a ViT [13] which takes all in information (noisy image, timestep embedding, textual embedding) as input tokens, which is different from the usual diffusion models [46] which processes conditional information using cross-attention layers throughout the depth of the model. We use the U-ViT proposed in [4] to tune adapters (deep prompts) in all the results of this paper. More specifically, we take an ImageNet [10] pre-trained conditional U-ViT (discard the ImageNet conditional tokens), and train deep prompts for different generation settings.

The popularity of diffusion models has also prompted researchers to investigate memorization [7], copyright protection [57] and privacy in diffusion models. [7] showed that diffusion models memorize training samples, and were able to successfully reconstruct the training data from the output of diffusion models, raising the privacy risk associated with such models. [57] provided a formalism for copyright protection in diffusion models using a less stringent version of differential privacy. They provided sampling algorithms to prevent the output of training samples from trained diffusion models after querying. To ensure privacy protected training of diffusion models, [12] proposed training diffusion models with differential privacy, however, they only provide results for toy datasets like MNIST [35]. [17] explores the common differential privacy idea of fine-tuning pre-trained models on private data, more specifically they fine-tune ImageNet pre-trained diffusion models on CIFAR datasets [33]. [16, 49] claim to provide methods to erase information/protect artists from diffusion models, however, their methods simply involve perturbing the weights of model to prevent generation of specific images, which does not address the critical issue that the weights of models still contain information about private sensitive copyright protected data. We aim to provide a method which enables us train multiple diffusion models (through prompts or adapters) on different shards of the data, and compose their predictions through an appropriate sampling mechanism. This enables us to continually add new models (new data sources) or remove data sources by simply dropping the corresponding shards.

In Section 3 we propose compartmentalized diffusion models, shows its derivations, along with computation of the weights Section 3.3. Then we discuss the architecture and the implementation details in Section 4, followed by the application of the proposed method in Section 5 and then providing our conclusion in Section 6.

	No Split	2-Split			4-Split			8-Split		
	(paragon)	Ours	Naïve	Single	Ours	Naïve	Single	Ours	Naïve	Single
<b>Pets[43]</b>	9.01	<b>8.72</b>	9.03	8.85	<b>9.42</b>	10.84	9.96	<b>9.53</b>	9.54	11.91
<b>CUB-200[9]</b>	3.73	<b>3.77</b>	5.04	3.85	<b>4.23</b>	5.37	4.51	<b>4.43</b>	13.01	6.71
<b>Stanf. Cars[32]</b>	5.05	4.7	6.14	<b>4.38</b>	5.79	8.68	<b>5.74</b>	<b>5.67</b>	35.05	6.47

Table 1: **Methods comparison for class conditional image generation.** We report, across various datasets, the FID score obtained with different methods to generate images starting from a compartmentalized model. We split each dataset uniformly across classes in multiple splits. Ideally the performance of the method should be close to the paragon performance of a non-compartmentalized model trained on all the data. We observe that for small number of shards the performance of the compartmentalized model can actually be better owing to the regularization effect of ensembling. FID score increase as we increase the number of splits as the models lose on synergistic information.

### 3 Compartmentalized Diffusion Models

Consider a dataset  $\mathcal{D} = \{D_1, \dots, D_n\}$  composed of  $n$  of different data sources  $D_n$ . The core idea of CDMs is to train separate models or adapters independently on each  $D_i$ , and compose them to obtain a model that behaves similarly to a model trained on the union  $\bigcup \mathcal{D}_i$  of all data. We now derive the correct way to do this.

There are different ways to arrive at the result. In the following, we start by summarizing the theory of Diffusion Models using the formalism of flow of vector fields following [37]. An advantage of this point of view is that it directly highlighting the key linearity properties that we exploit as well as the effect of compartmentalization on the sampling dynamics. Moreover, the same derivation holds not only for diffusion models, but more generally for any flow-based generative models. An alternative more restrictive derivation based on the connection between Diffusion Models and score function when using the common loss function is presented in the Appendix.

#### 3.1 Diffusion Models as Flows of Vector Fields

Let  $p(x)$  be the (unknown) ground-truth data distribution. The *forward probability path*  $p_t(x)$  of the diffusion model is defined as

$$p_t(x) = \int k_t(x, x_0)p(x_0)dx_0. \quad (1)$$

The probability kernel  $k_t(x, x_0)$  should be chosen in such a way that the path interpolates between the unknown ground-truth distribution  $p_0(x) = p(x)$  and a known distribution  $p_1(x) = N(0, I)$ . For example, in the Variance Preserving case, we pick  $k(x, x_0) = N(x|\alpha_t x_0, (1 - \alpha_t^2)I)$ , for some arbitrary scheduling  $\alpha_t$  such that  $\alpha_0 = 1$  and  $\alpha_1 = 0$ , which is readily seen to satisfy the condition.

The role of a diffusion model is to compute a vector field  $v_t(x)$  that generates the probability path. More precisely, let  $\phi_t(x)$  be the forward map obtained by following the vector field  $v_t(x)$ :

$$\frac{d}{dt}\phi_t(x) = v_t(\phi_t(x)) \quad (2)$$

We say that  $v_t(x)$  generates the probability path  $p_t(x)$ , if  $[\phi_t]_* p_0(x) = p_t(x)$ , that is, evolving the initial distribution following the flow gives the distribution at time  $t$ . This condition can be more conveniently expressed with the equivalent continuity equation [56]:

$$\frac{d}{dt}p_t(x) = \text{div}(p_t(x)v_t(x)). \quad (3)$$

Once such a vector field  $v_t(x)$  is obtained, to generate a new sample from the unknown distribution  $p_0(x)$  we simply need to sample  $\tilde{x}_1 \sim p_1(x)$  from the known distribution  $p_1(x) = N(0, I)$ , and follow the vector field in reverse, that is solving the ODE:

$$\frac{d}{dt}x_{1-t} = v_{1-t}(x_{1-t}) \quad (4)$$

with initial condition  $x_1 = \tilde{x}_1$ . The final point  $x_0$  will then be a sample from  $p_0(x) = p(x)$ . Diffusion models can be trained to approximate a vector field  $v_t$  that satisfies eq. (3) by training on a denoising objective [37], but we note that the particular objective used does not affect our method.

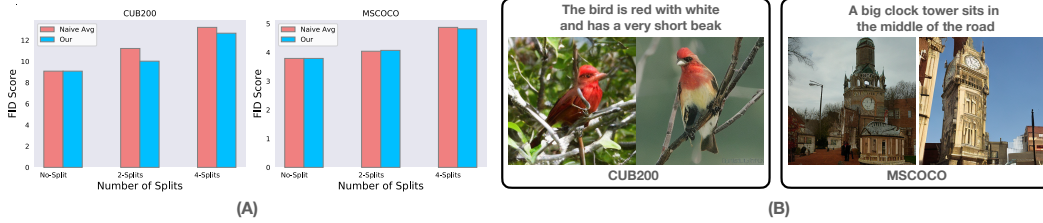


Figure 2: **Comparison for text-to-image fine-tuning and visualization:** (A) FID vs Number of splits for text-to-image generation for MSCOCO [36]. FID scores increases with splits due to loss of synergistic information. Our proposed method outperforms naive averaging. (B) Visualization of generated images along with the corresponding text caption. We fine-tune an ImageNet pre-trained class-conditional model using deep learnable prompts and adapters, and append the text caption (CLIP text embedding) along with input image tokens.

### 3.2 Compartmentalized Diffusion Models

Let us consider now the case where the data distribution  $p(x)$  is composed as a mixture of distributions:

$$p(x) = \lambda_1 p^{(1)}(x) + \dots + \lambda_n p^{(n)}(x),$$

such that the data from each training source  $D_i$  is sampled from its corresponding mixture component  $p^{(i)}(x)$ . Suppose that  $n$  independent diffusion models have been trained on each  $p^{(i)}(x)$  independently, leading to  $n$  different vector fields  $\{v_t^{(i)}\}_{i=1}^n$ . The question is whether we can combine these mixture-specific vector fields to generate a sample from the global distribution  $p^{(i)}(x)$ . To this end, we want to find a vector field  $v_t(x)$  that satisfies the continuity equation eq. (3).

First note that, by linearity of the forward path, in eq. (1) we have:

$$\begin{aligned} p_t(x) &= \int k_t(x, x_0) p(x_0) dx_0 = \int k_t(x, x_0) \left( \sum_i \lambda_i p^{(i)}(x_0) \right) dx_0 \\ &= \sum_{i=1}^n \lambda_i \int k_t(x, x_0) p^{(i)}(x_0) dx_0 = \sum_{i=1}^n \lambda_i p_t^{(i)}(x). \end{aligned} \quad (5)$$

Using this, we can write:

$$\begin{aligned} \frac{d}{dt} p_t(x) &= \sum_{i=1}^n \lambda_i \frac{d}{dt} p_t^{(i)}(x) = \sum_{i=1}^n \lambda_i \operatorname{div}(p_t^{(i)}(x) v_t^{(i)}(x)) \\ &= \operatorname{div} \left( \sum_{i=1}^n \lambda_i p_t^{(i)}(x) v_t^{(i)}(x) \right) \\ &= \operatorname{div} \left( p_t(x) \sum_{i=1}^n \lambda_i \frac{p_t^{(i)}(x)}{p_t(x)} v_t^{(i)}(x) \right) \end{aligned} \quad (6)$$

where in the second equality we used the fact that each  $v_t^{(i)}(t)$  satisfies its own continuity equation with respect to  $p_t^{(i)}(x)$ . From eq. (6) we then see that choosing

$$v_t(x) = \sum_{i=1}^n \lambda_i \frac{p_t^{(i)}(x)}{p_t(x)} v_t^{(i)}(x)$$

satisfies the continuity equation for  $p_t(x)$ . We summarize this result in the following.

**Proposition 3.1.** Let  $\{p^{(i)}(x)\}_{i=1}^N$  be probability distributions, and let  $v_t^{(i)}(x)$  be the output (vector field) of a Diffusion Model trained on  $p^{(i)}(x)$ . Then,

$$v_t(x) = \sum_{i=1}^n \lambda_i w_i(x, t) v_t^{(i)}(x),$$

where  $w_i(x, t) = \frac{p_t^{(i)}(x)}{p_t(x)}$  is a valid flow for the mixture  $p(x) = \lambda_1 p^{(1)}(x) + \dots + \lambda_n p^{(n)}(x)$ .

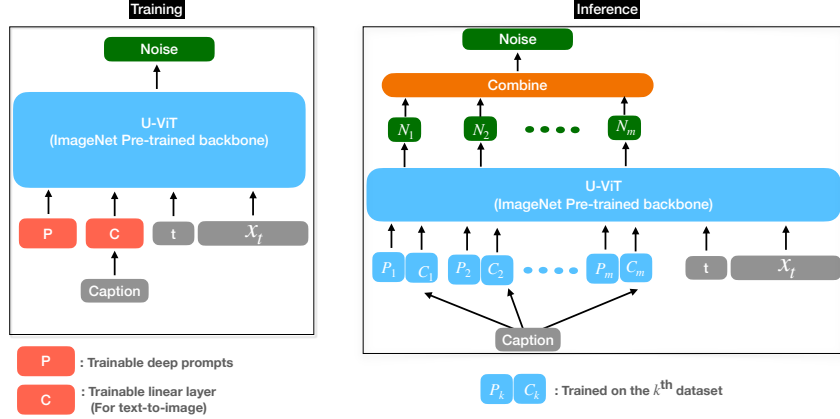


Figure 3: **Diagram of model architecture.** We use a vision transformer (U-ViT) which takes as input; the noisy image, timestep embedding, any conditional information (like textual captions), and the trainable deep prompts. **(Left)** We train deep prompts keeping the backbone fixed for different data distributions. The backbone is pre-trained on ImageNet for class-conditional image generation. We discard the class conditional ImageNet pre-trained tokens, and instead append new learnable prompts. For unconditional generation, we train one set of deep prompts for the entire dataset, while for class-conditional generation we train one set of deep prompts for each class. To adapt this model to text-to-image generation, we also train a linear transformation layer, which transforms the CLIP textual embeddings to the same space as the input image. **(Right)** During inference, we take prompts trained on multiple sources of data and combine them using the weights obtained in section 3.3.

Proposition 3.1 highlights an important point. While we can correctly sample from a combined distribution by simply averaging the outputs of diffusion models trained on each component individually, *naive ensembling of the models is incorrect*: simply using a weighted average  $\sum_i \lambda_i v_{(i)}(x)$  of the output of each model will not yield the correct result (see Figure 1, Figure 2, Table 1, Naive averaging performs worse compared to our method in Proposition 3.1). Rather, each model’s output needs to be weighted by an additional term  $w_i(x, t) = p_t^{(i)}(x)/p_t(x)$  which depends both on the time  $t$  and the current noisy sample  $x_t$ .

### 3.3 Computing the weights

This additional term indeed has an intuitive interpretation. Let  $x_0 \sim p(x) = \sum_i \lambda_i p^{(i)}(x)$  be a sample from the mixture distribution, and let  $z \in \{1, \dots, n\}$  be a discrete random variable which tells us the index of the mixture component that generated the sample (so that  $p(x|z = i) = p^{(i)}(x)$  and  $p(x) = \sum_i p(x|z = i)p(z = i)$ ). Then, by Bayes’s rule, one readily sees that

$$p_t(z = i|x) = \frac{p_t^{(i)}(x)}{p_t(x)}.$$

That is, the additional weighting factor for each model can be interpreted as the probability that the current noisy sample  $x_t$  originated from the data distribution used to train that model. To illustrate the behavior (see Figure 1), consider the case where  $p^{(1)}(x)$  and  $p^{(2)}(x)$  are disjoint (for example, images of pets and flowers respectively). At the beginning of the reverse diffusion, due to the amount of noise the sample is equally likely to be generated from either distribution, and both will have similar weight. As the time increases and more details are added to the sample, the image will increasingly be more likely to be either a pet or a flower. Correspondingly the generated image should draw only from the relevant domains, whereas using others would force the model to generate images of flowers by inductively combining images of pets (Figure 1).

This interpretation also gives us a way to compute  $\frac{p_t^{(i)}(x)}{p_t(x)}$ . In principle, one could estimate both  $p_t^{(i)}(x)$  and  $p_t(x)$  using the diffusion model itself (see Appendix), however this is computationally expensive. On the other hand,  $p_t(z = i|x)$  is simple to estimate directly with a small auxiliary model. Let  $f(x, t)$  be a  $n$ -way classification network that takes as input a noisy image  $x$  and a time-step  $t$  and outputs

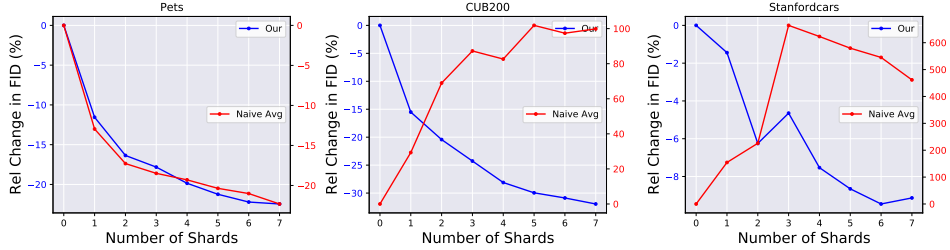


Figure 4: **Forgetting/Continual Learning:** Relative change (wrt single shard) in the FID score as we continually add more shards (class-conditional generation with 8-splits). FID scores for our method continuously decreases as we add more shards compared to naive averaging which may result in incorrect mixture of vector fields.

a softmax. To train the network, generate pairs  $\{(x_i, k_i)\}_{i=1}^N$  where  $k_i \sim 1, \dots, n$  is a random component index and  $x_i \sim N(x|\alpha_t x_0, (1 - \alpha_t^2)I)$ ,  $x_0 \sim D_{k_i}$  is obtained by sampling a training image from the corresponding dataset  $D_{k_i}$  and adding noise to it. The network is trained with the cross-entropy loss to predict  $k_i$  given  $x_i$  and  $t$ . Then, at convergence  $f(x, t) = \left(\frac{p_t^{(1)}(x)}{p_t(x)}, \dots, \frac{p_t^{(n)}(x)}{p_t(x)}\right)$ .

**Proposition 3.2.** Let  $f_w$  be a classifier trained as described. Then

$$f_w(x, t)_i = w_i(x, t)$$

where  $w_i(x, t)$  is as in Proposition 3.1.

## 4 Architecture and Implementation

In practice, rather than training a separate diffusion model with hundreds of millions of parameters for each data distribution, we fine-tune deep prompts (adapters) on a pre-trained backbone. This further reduces the number of trainable parameter and inference cost, since most of the computations will be shared with the backbone diffusion model. We use latent diffusion models (as used in U-ViT [4] to generate  $256 \times 256$  images). The above strategy to compose diffusion models can be applied to combine any set of diffusion models, even if implemented with a different architecture, as long as the latent space and the forward process used is the same (which is usually the case). For example, one may train a separate model on each component. However, this is inefficient since both the storage and the inference cost would increase linearly with the number of components to combine.

**Prompt Tuning** We propose a more efficient approach based on prompt tuning [28, 6]. Given a core model trained on a core set, prompt tuning can be used to fine-tune the model on a new data distribution. We use an ImageNet pre-trained U-ViT [4], as our core model. The U-ViT model takes all the information to process as input tokens (noisy image, timestep embedding, conditional information) and generates the predicted noise, compared to other methods [46] which uses cross-attention layers throughout the depth. *Unconditional Generation:* We train one set of prompts corresponding to each data distribution. *Class-conditional Generation:* We train one set of prompts for each class per data distribution. *Text-to-Image Generation* (see Figure 2): We again train one set of deep prompts for each data distribution, however, unlike the previous cases, we also need to condition the model with text captions. We use the CLIP textual embeddings [44] to encode the text. However, the textual embeddings may not lie in the same space (also dimensionality) as the input image embeddings, so we train an additional linear layer to transform the CLIP embeddings and prompt these transformed embeddings to all the layers of the U-ViT (see Figure 3).

**Classifier** Instead of training a separate classifier for predicting the composition weights (Proposition 3.2), we simply attach an attention layer after middle block of U-ViT for each data distribution. This attention block provides a single number corresponding to the contribution of each model towards the final ensemble. We softmax these predictions to obtain composition weights from Proposition 3.1. Since the input to the attention block is a function  $t$  and  $x_t$ , during inference, we obtain the time-dependent composition weights (using the attention block) for free during the forward pass through U-ViT while predicting the noise for the next step. The complete architecture for training and inference is described in Figure 3.

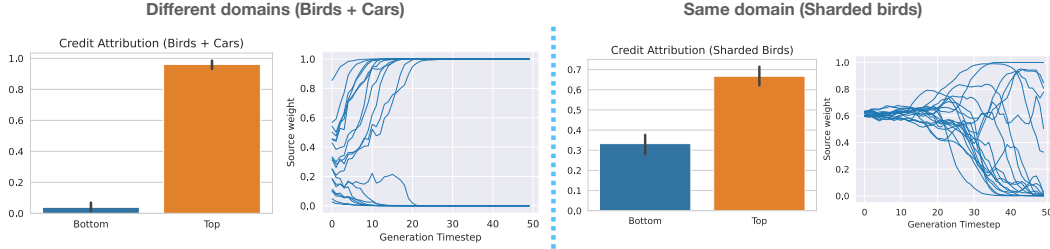


Figure 5: **Credit attribution.** Show average credit attribution when shards are from different domains (CUB200 [9] and Cars [32]) and when shards are uniform split of the same domain.

## 5 Applications

**À-la-carte diffusion models.** [6] introduces the notion of *à-la-carte learning* as a uniform solution to several common problems in large-scale training such as per-user model customization, machine unlearning, continual learning. Let  $f$  be a model and let  $\mathcal{D} = \{D_1, \dots, D_n\}$  be a variable collection of data sources. In *à-la-carte learning* a user at inference time can specify a subset  $S \subset \mathcal{D}$  and receive a personalized *à-la-carte* output  $f(x, S)$  which, critically, depends *only* on the data source  $S_i \in S$ . By selecting  $S$  appropriately, as described next, different problem may be addressed. The challenge is how to allow selecting different  $S$  at inference time without pre-training a model on all  $2^n$  possible combinations of sources the user can select. CDMs are a direct solution to this problem in the case of diffusion models. Let  $\{f_i(x, t)\}_{i=1}^N$  be diffusion models trained individually on each  $D_i$ . Given a user selected  $S = \{D_{s_1}, \dots, D_{s_k}\}$ , we simply need to select the corresponding models  $\{f_{s_i}\}_{i=1}^k$  and combine them using Proposition 3.1.

**Forgetting.** Owners of the training data may, at any point, modify their sharing preferences leading to a shrinking set  $S$  of usable sources. When this happens, all information about that data needs to be removed from the model. However, the large amount of current state-of-the-art diffusion models precludes re-training on the remaining data as a viable strategy. Compartmentalized models such as CDMs allow for a simple solution to the problem: if a data source  $D_i$  is removed, we only need to remove the corresponding model  $f_i$  to remove all information about it. Moreover, if only a subset of a training source is removed, it is only necessary to retrain the corresponding model. We show that increasing the number of splits does not increase the FID scores after composition (Table 1, Figure 2) which is critical for forgetting as it enables easy removals of shards without significantly losing performance. Figure 4 shows the relative change in the FID score as we drop shards.

**Continual Learning.** The data sources  $D_i$  may represent additional batches of training data that are acquired incrementally. Retraining the model from scratch every time new data is acquired, or fine-tuning an existing model, which brings the risk of catastrophic forgetting, is not desirable in this case. With CDMs, one can simply train an additional model  $f_i$  on  $D_i$  and compose it with the previous models. In Figure 4 we show that adding more shards in a continual fashion improves the FID score relative to a single shard. Also, simple naive averaging over the shards will result in incorrect mixture of vector fields which can be avoided by the method proposed in Proposition 3.1.

**Differential Privacy (DP).** Protecting copyrights of a training sample is an important privacy concern while training large scale diffusion models. [57] proposed a method for protecting the copyrights of specific samples within the training set. Their method is a weaker condition than differential privacy [15], and is similar to differential privacy when copyright protection is extended to all the training samples. Towards this end, we fine-tune the text-to-image prompt based model (see Figure 3) with differential privacy, more specifically DP-SGD [1]. In Figure 6 we show that DP degrades the quality of the generated images, and also weakens the association between the textual captions and generated images, while providing copyright protection according to the framework proposed in [57] (as DP is more stricter). To the best of our knowledge this is the first work to train text-to-image diffusion models with DP on large-scale datasets ( $(256 \times 256)$  images).

**Measuring contribution of individual sources.** Let  $x_0$  be a sample generated solving the ODE eq. (4) starting from an initial  $x_1 \sim p_1(x)$ . The likelihood of a generated image can then be computed





Figure 6: **Differential Privacy** Generated images from our DP text-to-image model ( $\epsilon = 3$ ,  $\epsilon = 8$  and non-private) trained on MSCOCO [36]. Differential privacy weakens the dependence of the generated images on the input captions and degrades the quality of images ( $\epsilon = \infty$ : non-private training ensures direct correlation between captions and images which is weakened with private training). DP training also ensures copyright protection for all training samples [57].

as

$$\log p_1(x_1) - \log p(x_0) = - \int_0^1 \text{div}(v(x_t)) dt,$$

that is, the divergence of the score function integrated along the path. In the case of a CDM, this likelihood can further be decomposed as:

$$\log p_1(x_1) - \log p_0(x_0) = \sum_i \lambda_i \int \text{div}(w_i(x_t, t) v_t^{(i)}(x_t)) dt = \sum_i \lambda_i L_i$$

where  $L_i$  can be interpreted as the contribution to each component of the model to the total likelihood.

Using this, we can quantify the credit  $C_i$  of the data source  $D_i$  as:

$$C_i = \frac{\lambda L_i}{\sum_{j=1}^n \lambda_j L_j}.$$

We note that while  $\sum_i \lambda_i L_i$  is the likelihood assigned by the CDM to the the generated sample, one cannot interpret the individual  $L_i$  as the likelihood assigned by each submodel. In Figure 5 we show that when shards belongs to different distributions the credit attribution is correctly more skewed (generated image belongs to one distribution) compared to similar distributions which has a more uniform attribution (since all distributions are similar). The composition weights for different domains at inference start with similar values and change rapidly within the first 10 generation steps (see Figure 5 left). For the case of same domains the weights start with similar values and maintain them until almost half generation is complete before selecting one split (Figure 5 right).

## 6 Conclusion

Data protection is an increasingly arduous task as the volume of training data needed to train massive AI models increases. While techniques to manage privacy and attribution have been demonstrated for a variety of model architectures, mostly at relatively small scale, up to now it was not possible to directly apply them to Diffusion Models. We present the first method to compose such models, and illustrate its use in customized model inference (‘a-la-carte), selective forgetting, continual learning, and differential privacy. We show that we can train compartmentalized diffusion models using deep learnable prompts (or adapters) to model different data distributions Figure 3. These prompts are memory efficient with enough expressivity to generate realistic large-scale images. In Figure 2 we demonstrate the strength of such prompts in generating images from textual captions, despite the UViT model never having encountered textual conditioning while pre-training. Thus all the information pertaining to text/captions is only injected into the deep prompts while fine-tuning. This idea is further explored for training differentially private text-to-image diffusion models which enables copyright protection during training and inference.

## References

- [1] Martin Abadi, Andy Chu, Ian Goodfellow, H Brendan McMahan, Ilya Mironov, Kunal Talwar, and Li Zhang. Deep learning with differential privacy. In *Proceedings of the 2016 ACM SIGSAC conference on computer and communications security*, pages 308–318, 2016.
- [2] Alessandro Achille, Aditya Golatkar, Avinash Ravichandran, Marzia Polito, and Stefano Soatto. Lqf: Linear quadratic fine-tuning. In *Proceedings of the IEEE/CVF Conference on Computer Vision and Pattern Recognition*, pages 15729–15739, 2021.
- [3] Brian DO Anderson. Reverse-time diffusion equation models. *Stochastic Processes and their Applications*, 12(3):313–326, 1982.
- [4] Fan Bao, Chongxuan Li, Yue Cao, and Jun Zhu. All are worth words: a vit backbone for score-based diffusion models. *arXiv preprint arXiv:2209.12152*, 2022.
- [5] Lucas Bourtole, Varun Chandrasekaran, Christopher A Choquette-Choo, Hengrui Jia, Adelin Travers, Baiwu Zhang, David Lie, and Nicolas Papernot. Machine unlearning. In *2021 IEEE Symposium on Security and Privacy (SP)*, pages 141–159. IEEE, 2021.
- [6] Benjamin Bowman, Alessandro Achille, Luca Zancato, Matthew Trager, Pramuditha Perera, Giovanni Paolini, and Stefano Soatto. \a-la-carte prompt tuning (apt): Combining distinct data via composable prompting. *arXiv preprint arXiv:2302.07994*, 2023.
- [7] Nicholas Carlini, Jamie Hayes, Milad Nasr, Matthew Jagielski, Vikash Sehwal, Florian Tramèr, Borja Balle, Daphne Ippolito, and Eric Wallace. Extracting training data from diffusion models. *arXiv preprint arXiv:2301.13188*, 2023.
- [8] Rishav Chourasia, Neil Shah, and Reza Shokri. Forget unlearning: Towards true data-deletion in machine learning. *arXiv preprint arXiv:2210.08911*, 2022.
- [9] C.Wah, S.Branson, P.Welinder, P.Perona, and S.Belongie. Technical report cns-tr-2011-001, california institute of technology. *Caltech*, 2011.
- [10] Jia Deng, Wei Dong, Richard Socher, Li-Jia Li, Kai Li, and Li Fei-Fei. Imagenet: A large-scale hierarchical image database. In *2009 IEEE conference on computer vision and pattern recognition*, pages 248–255. Ieee, 2009.
- [11] Prafulla Dhariwal and Alexander Nichol. Diffusion models beat gans on image synthesis. *Advances in Neural Information Processing Systems*, 34:8780–8794, 2021.
- [12] Tim Dockhorn, Tianshi Cao, Arash Vahdat, and Karsten Kreis. Differentially private diffusion models. *arXiv preprint arXiv:2210.09929*, 2022.
- [13] Alexey Dosovitskiy, Lucas Beyer, Alexander Kolesnikov, Dirk Weissenborn, Xiaohua Zhai, Thomas Unterthiner, Mostafa Dehghani, Matthias Minderer, Georg Heigold, Sylvain Gelly, et al. An image is worth 16x16 words: Transformers for image recognition at scale. *arXiv preprint arXiv:2010.11929*, 2020.
- [14] Yonatan Dukler, Benjamin Bowman, Alessandro Achille, Aditya Golatkar, Ashwin Swaminathan, and Stefano Soatto. Safe: Machine unlearning with shard graphs. *arXiv preprint arXiv:2304.13169*, 2023.
- [15] Cynthia Dwork, Aaron Roth, et al. The algorithmic foundations of differential privacy. *Foundations and Trends® in Theoretical Computer Science*, 9(3–4):211–407, 2014.
- [16] Rohit Gandikota, Joanna Materzynska, Jaden Fiotto-Kaufman, and David Bau. Erasing concepts from diffusion models. *arXiv preprint arXiv:2303.07345*, 2023.
- [17] Sahra Ghalebikesabi, Leonard Berrada, Sven Gowal, Ira Ktena, Robert Stanforth, Jamie Hayes, Soham De, Samuel L Smith, Olivia Wiles, and Borja Balle. Differentially private diffusion models generate useful synthetic images. *arXiv preprint arXiv:2302.13861*, 2023.
- [18] Antonio Ginart, Melody Guan, Gregory Valiant, and James Y Zou. Making ai forget you: Data deletion in machine learning. *Advances in neural information processing systems*, 32, 2019.
- [19] Aditya Golatkar, Alessandro Achille, Avinash Ravichandran, Marzia Polito, and Stefano Soatto. Mixed-privacy forgetting in deep networks. In *Proceedings of the IEEE/CVF Conference on Computer Vision and Pattern Recognition (CVPR)*, pages 792–801, June 2021.
- [20] Aditya Golatkar, Alessandro Achille, and Stefano Soatto. Eternal sunshine of the spotless net: Selective forgetting in deep networks. In *Proceedings of the IEEE/CVF Conference on Computer Vision and Pattern Recognition (CVPR)*, June 2020.

- [21] Aditya Golatkar, Alessandro Achille, and Stefano Soatto. Forgetting outside the box: Scrubbing deep networks of information accessible from input-output observations. In *European Conference on Computer Vision*, pages 383–398. Springer, 2020.
- [22] Aditya Golatkar, Alessandro Achille, Yu-Xiang Wang, Aaron Roth, Michael Kearns, and Stefano Soatto. Mixed differential privacy in computer vision. In *Proceedings of the IEEE/CVF Conference on Computer Vision and Pattern Recognition*, pages 8376–8386, 2022.
- [23] Ian Goodfellow, Jean Pouget-Abadie, Mehdi Mirza, Bing Xu, David Warde-Farley, Sherjil Ozair, Aaron Courville, and Yoshua Bengio. Generative adversarial networks. *Communications of the ACM*, 63(11):139–144, 2020.
- [24] Chuan Guo, Tom Goldstein, Awni Hannun, and Laurens Van Der Maaten. Certified data removal from machine learning models. *arXiv preprint arXiv:1911.03030*, 2019.
- [25] Varun Gupta, Christopher Jung, Seth Neel, Aaron Roth, Saeed Sharifi-Malvajerdi, and Chris Waites. Adaptive machine unlearning. *Advances in Neural Information Processing Systems*, 34:16319–16330, 2021.
- [26] Jonathan Ho, William Chan, Chitwan Saharia, Jay Whang, Ruiqi Gao, Alexey Gritsenko, Diederik P Kingma, Ben Poole, Mohammad Norouzi, David J Fleet, et al. Imagen video: High definition video generation with diffusion models. *arXiv preprint arXiv:2210.02303*, 2022.
- [27] Jonathan Ho, Ajay Jain, and Pieter Abbeel. Denoising diffusion probabilistic models. *Advances in Neural Information Processing Systems*, 33:6840–6851, 2020.
- [28] Menglin Jia, Luming Tang, Bor-Chun Chen, Claire Cardie, Serge Belongie, Bharath Hariharan, and Ser-Nam Lim. Visual prompt tuning. In *Computer Vision–ECCV 2022: 17th European Conference, Tel Aviv, Israel, October 23–27, 2022, Proceedings, Part XXXIII*, pages 709–727. Springer, 2022.
- [29] Tero Karras, Miika Aittala, Timo Aila, and Samuli Laine. Elucidating the design space of diffusion-based generative models. *arXiv preprint arXiv:2206.00364*, 2022.
- [30] Diederik P Kingma and Max Welling. Auto-encoding variational bayes. *arXiv preprint arXiv:1312.6114*, 2013.
- [31] Korbinian Koch and Marcus Soll. No matter how you slice it: Machine unlearning with sisa comes at the expense of minority classes. In *First IEEE Conference on Secure and Trustworthy Machine Learning*, 2023.
- [32] Jonathan Krause, Michael Stark, Jia Deng, and Li Fei-Fei. 3d object representations for fine-grained categorization. In *Proceedings of the IEEE international conference on computer vision workshops*, pages 554–561, 2013.
- [33] Alex Krizhevsky, Geoffrey Hinton, et al. Learning multiple layers of features from tiny images. *Toronto, ON, Canada*, 2009.
- [34] Vinayshekhar Bannihatti Kumar, Rashmi Gangadharaiah, and Dan Roth. Privacy adhering machine un-learning in nlp. *arXiv preprint arXiv:2212.09573*, 2022.
- [35] Yann LeCun, Corinna Cortes, and Chris Burges. Mnist handwritten digit database. *Dataset*, 2010.
- [36] Tsung-Yi Lin, Michael Maire, Serge Belongie, James Hays, Pietro Perona, Deva Ramanan, Piotr Dollár, and C Lawrence Zitnick. Microsoft coco: Common objects in context. In *Computer Vision–ECCV 2014: 13th European Conference, Zurich, Switzerland, September 6–12, 2014, Proceedings, Part V 13*, pages 740–755. Springer, 2014.
- [37] Yaron Lipman, Ricky TQ Chen, Heli Ben-Hamu, Maximilian Nickel, and Matt Le. Flow matching for generative modeling. *arXiv preprint arXiv:2210.02747*, 2022.
- [38] Cheng Lu, Yuhao Zhou, Fan Bao, Jianfei Chen, Chongxuan Li, and Jun Zhu. Dpm-solver: A fast ode solver for diffusion probabilistic model sampling in around 10 steps. *arXiv preprint arXiv:2206.00927*, 2022.
- [39] Cheng Lu, Yuhao Zhou, Fan Bao, Jianfei Chen, Chongxuan Li, and Jun Zhu. Dpm-solver++: Fast solver for guided sampling of diffusion probabilistic models. *arXiv preprint arXiv:2211.01095*, 2022.

- [40] Eyal Molad, Eliahu Horwitz, Dani Valevski, Alex Rav Acha, Yossi Matias, Yael Pritch, Yaniv Leviathan, and Yedid Hoshen. Dreamix: Video diffusion models are general video editors. *arXiv preprint arXiv:2302.01329*, 2023.
- [41] Seth Neel, Aaron Roth, and Saeed Sharifi-Malvajerdi. Descent-to-delete: Gradient-based methods for machine unlearning. In *Algorithmic Learning Theory*, pages 931–962. PMLR, 2021.
- [42] Edward Nelson. *Dynamical theories of Brownian motion*. Princeton university press, 1967.
- [43] Omkar M Parkhi, Andrea Vedaldi, Andrew Zisserman, and CV Jawahar. Cats and dogs. In *2012 IEEE conference on computer vision and pattern recognition*, pages 3498–3505. IEEE, 2012.
- [44] Alec Radford, Jong Wook Kim, Chris Hallacy, Aditya Ramesh, Gabriel Goh, Sandhini Agarwal, Girish Sastry, Amanda Askell, Pamela Mishkin, Jack Clark, et al. Learning transferable visual models from natural language supervision. In *International conference on machine learning*, pages 8748–8763. PMLR, 2021.
- [45] Aditya Ramesh, Prafulla Dhariwal, Alex Nichol, Casey Chu, and Mark Chen. Hierarchical text-conditional image generation with clip latents. *arXiv preprint arXiv:2204.06125*, 2022.
- [46] Robin Rombach, Andreas Blattmann, Dominik Lorenz, Patrick Esser, and Björn Ommer. High-resolution image synthesis with latent diffusion models. In *Proceedings of the IEEE/CVF Conference on Computer Vision and Pattern Recognition*, pages 10684–10695, 2022.
- [47] Olaf Ronneberger, Philipp Fischer, and Thomas Brox. U-net: Convolutional networks for biomedical image segmentation. In *Medical Image Computing and Computer-Assisted Intervention—MICCAI 2015: 18th International Conference, Munich, Germany, October 5-9, 2015, Proceedings, Part III 18*, pages 234–241. Springer, 2015.
- [48] Ayush Sekhari, Jayadev Acharya, Gautam Kamath, and Ananda Theertha Suresh. Remember what you want to forget: Algorithms for machine unlearning. *Advances in Neural Information Processing Systems*, 34:18075–18086, 2021.
- [49] Shawn Shan, Jenna Cryan, Emily Wenger, Haitao Zheng, Rana Hanocka, and Ben Y Zhao. Glaze: Protecting artists from style mimicry by text-to-image models. *arXiv preprint arXiv:2302.04222*, 2023.
- [50] Jiaming Song, Chenlin Meng, and Stefano Ermon. Denoising diffusion implicit models. *arXiv preprint arXiv:2010.02502*, 2020.
- [51] Yang Song, Conor Durkan, Iain Murray, and Stefano Ermon. Maximum likelihood training of score-based diffusion models. *Advances in Neural Information Processing Systems*, 34:1415–1428, 2021.
- [52] Yang Song and Stefano Ermon. Improved techniques for training score-based generative models. *Advances in neural information processing systems*, 33:12438–12448, 2020.
- [53] Yang Song, Sahaj Garg, Jiaxin Shi, and Stefano Ermon. Sliced score matching: A scalable approach to density and score estimation. In *Uncertainty in Artificial Intelligence*, pages 574–584. PMLR, 2020.
- [54] Yang Song, Jascha Sohl-Dickstein, Diederik P Kingma, Abhishek Kumar, Stefano Ermon, and Ben Poole. Score-based generative modeling through stochastic differential equations. *arXiv preprint arXiv:2011.13456*, 2020.
- [55] Enayat Ullah, Tung Mai, Anup Rao, Ryan A Rossi, and Raman Arora. Machine unlearning via algorithmic stability. In *Conference on Learning Theory*, pages 4126–4142. PMLR, 2021.
- [56] Cédric Villani et al. *Optimal transport: old and new*, volume 338. Springer, 2009.
- [57] Nikhil Vyas, Sham Kakade, and Boaz Barak. Provable copyright protection for generative models. *arXiv preprint arXiv:2302.10870*, 2023.
- [58] Haonan Yan, Xiaoguang Li, Ziyao Guo, Hui Li, Fenghua Li, and Xiaodong Lin. Arcane: An efficient architecture for exact machine unlearning. In *Proceedings of the Thirty-First International Joint Conference on Artificial Intelligence, IJCAI-22*, pages 4006–4013, 2022.
- [59] Sihao Yu, Fei Sun, Jiafeng Guo, Ruqing Zhang, and Xueqi Cheng. Legonet: A fast and exact unlearning architecture. *arXiv preprint arXiv:2210.16023*, 2022.

## A Implementation Details

We use transformer based diffusion models for all the experiments performed in the paper. More specifically we use the U-ViT architecture proposed in [4], whose code can be publicly found here: <https://github.com/baofff/U-ViT>. In all the experiments we train prompts (adapters) to learn the data distribution. We use an ImageNet pretrained class-conditional model as the backbone and learn prompts (adapters) to model the data distribution. We use the Adam optimizer with a learning rate of 0.1 for all our non-differential privacy experiments, and learning rate of 1 for the differential privacy experiments. We do not use weight decay while fine-tuning and use a batch-size of 256 for all non differential privacy experiments. Since all the experiments are performed on  $256 \times 256$  sized images, we use latent diffusion models where we cache the latent embeddings for the entire dataset to speed up training.

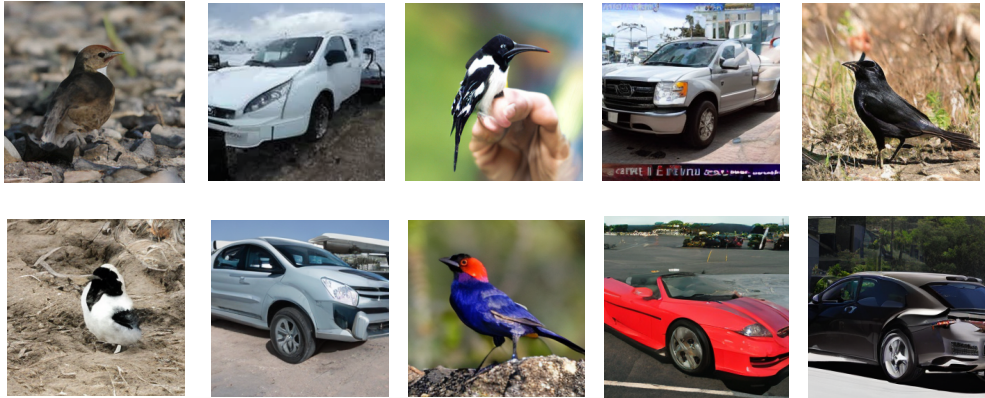
For unconditional image generation we train one set of deep prompts (deep prompts: prompts appended to all the layers of a the network, see [28]) for the entire distribution. We use a prompt length of 256 tokens, and train for 800 epochs.

For class-conditional image generation, we train one set of deep prompts for each class. Since we train class-wise prompts, we use a prompt length of 8 tokens, and again train for 800 epochs.

For text-to-image generation, we use a prompt length of 64 along with a linear transformation layer which projects the CLIP embeddings into the input token space, and also a parallel adapter across each feedforward layer. The FID scores are robust to the number of prompt tokens and we choose them such that the number of parameters are approximately the same across different settings. For differentially private learning we try two values of  $\epsilon = 3, 8$ , we use a batch-size of 8192 with a learning rate of 1.

## B Additional Figures

Diffusion model composition with our method: Birds + Cars



Diffusion model composition with naive averaging: Birds + Cars



Figure 7: Diffusion model composition with our method vs naive averaging

A baseball player swinging a bat at a ball



Figure 8: Text-to-Image generation with a prompt (adapter) based model trained on MS-COCO

A colorful bird is perched on branch



Figure 9: Text-to-Image generation with a prompt (adapter) based model trained on MS-COCO

A stuffed teddy bear sitting on a stool



Figure 10: Text-to-Image generation with a prompt (adapter) based model trained on MS-COCO

A long empty road way surrounded by wild plants



Figure 11: Text-to-Image generation with a prompt (adapter) based model trained on MS-COCO



Unconditional Pets generation

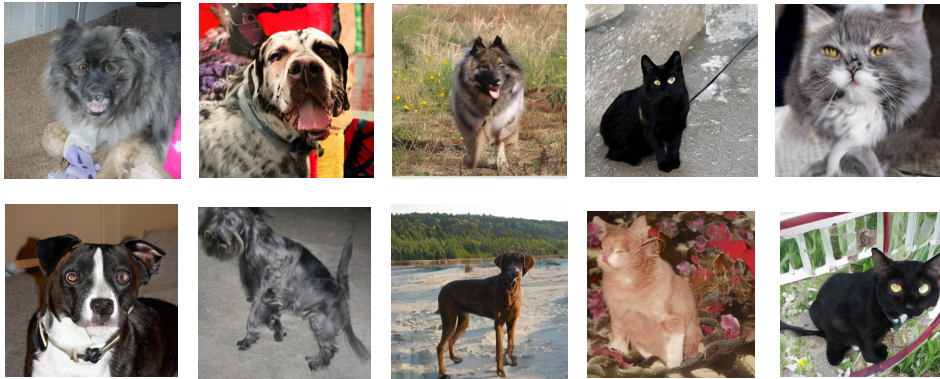


Figure 12: Unconditional image generation with a prompt (adapter) based model trained on Oxford-Pets

Unconditional Birds generation



Figure 13: Unconditional image generation with a prompt (adapter) based model trained on CUB200